Appendix C

Rheological measurements with polyester particles

C.1 Motivation

To study the effect of higher density ratio as well as particles' size and shape effect, torque measurements using polyester particles were made. As described in Section 2.2 polyester particles are 1.33 times denser than the polystyrene particles used in the experiments described in Chapter 4 and 5. If the suspending liquid is water, the density ratio is 1.4. For these experiments the rough walls are the same as the ones used for the experiments with polystyrene (polystyrene particles glued to the walls). A description of experiments with polyester particles and three different suspending liquids is presented in the next section.

C.2 Polyester particles with $\rho_p/\rho = 1.4$

Figure C.1 shows the measured torque for loading fractions of 10 and 20% for polyester particles immersed in water ($\rho_p/\rho = 1.4$). The corresponding measured torques for pure water are also shown in Figure C.1. At low shear rates, the measured torques for the liquid-solid flow coincide with the measured torques for pure liquid. Approximately at $\dot{\gamma} = 60\ s^{-1}$, the measured torques start deviating from the pure liquid ones. Polyester particles are smaller than the polystyrene particles ($d = 2.93$ mm) and have a higher random loose packing ($\phi_{RLP} = 0.593$). When settled, the polyester particles do not reach the test section for loading fractions of 10 and 20%. For this reason the measured torques at low shear rates coincide with the pure fluid measurements. The torques increase in a non-linear way with shear rate.

Figure C.2 presents the measured torques for higher loading fractions of 30, 40 , and 50%. Unlike the results for polystyrene particles (see Figure 4.13), the torques not always increase with shear rate. For the highest loading fractions tested (40 and 50%), the measured torques show a drop for

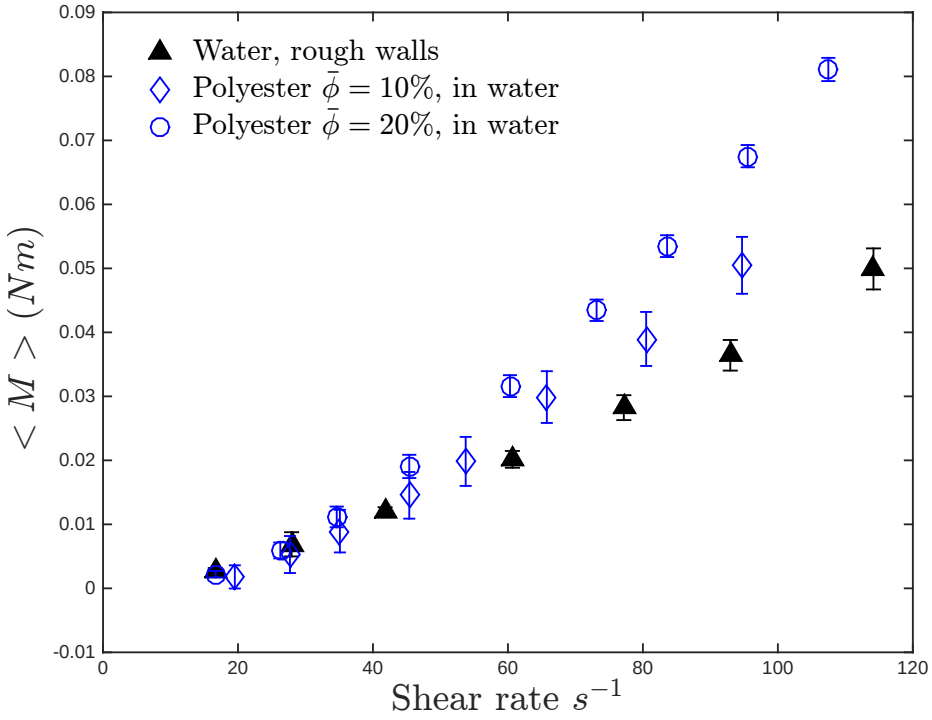

Figure C.1: Measured torques for polyester particles with $\rho_p/\rho = 1.4$ and for pure water. Error bars represents the combined uncertainty of the measurements.

shear rates higher than 30 s^{-1}. For $\bar{\phi} = 50\%$ the torques continue to decrease with shear rates. For $\bar{\phi} = 40\%$ the torques appear to reach a plateau for shear rates higher than 100 s^{-1}. For $\bar{\phi} = 30\%$, the torques show a slight drop at shear rates around 20 s^{-1} and they start increasing at shear rates around 60 s^{-1}. Visualizations of the flow show that these behaviors are a result of centripetal forces. For these higher density ratios, the centripetal forces due to the rotation of the outer cylinder are higher than the forces presented for lower density ratios. Under such forces, the particles are pushed away from the inner cylinder. Results of the visualization of the flow for polyester particles are presented later in Section C.5.

Figure C.3 shows the measured torques normalized with the corresponding laminar torques predicted from laminar theory. For the lowest loading fractions of 10 and 20, only the normalized torques corresponding to the Stokes number where particles reach the test section are shown. The normalized torques show a similar behavior as the case with settling polystyrene particles where $M/M_{laminar}$ increases for loading fractions lower than 30% and decreases for higher loading fractions. For $\bar{\phi} = 30\%$, the ratio of torques increases for Stokes numbers above 60. For $\bar{\phi} = 40\%$, the normalized torques appear to reach a plateau at Stokes numbers above 100. The only difference in behavior is that for $\bar{\phi} = 50\%$, the ratio of torques does not seem to reach a plateau and continues to decrease with the shear rate.

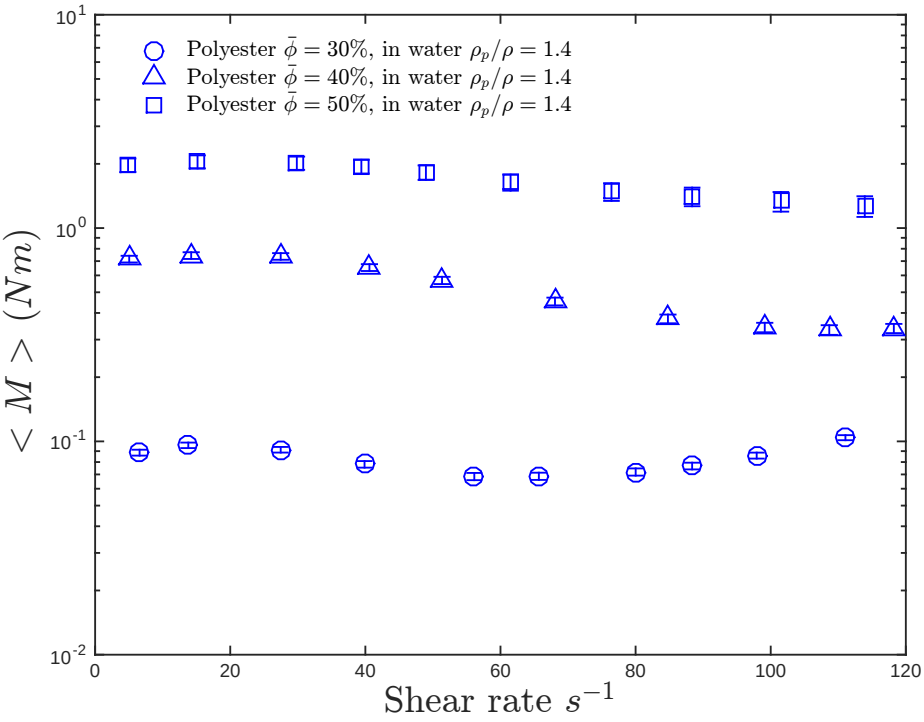

Figure C.2: Measured torques for polyester particles with $\rho_p/\rho = 1.4$ and for pure water. The loading fractions shown are 30, 40, and 50%. Error bars represents the combined uncertainty of the measurements.

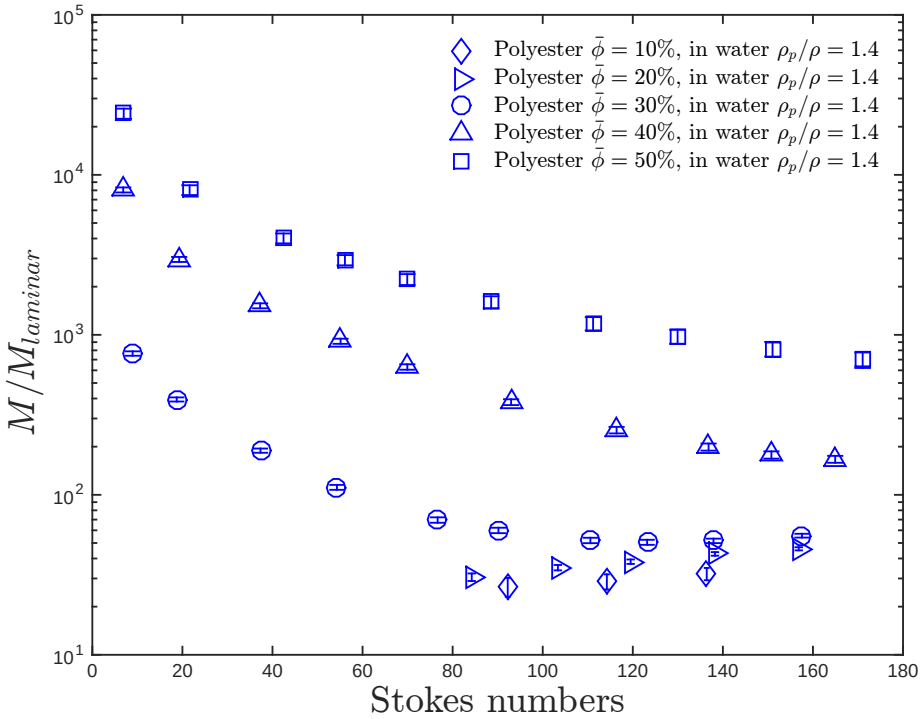

Figure C.3: Normalized torques for polyester particles with $\rho_p/\rho = 1.4$ and $\bar{\phi} = 10, 20, 30, 40$, and 50%. Only the results for the case where the particles reach the test section are shown. Error bars represents the combined uncertainty of the measurements.

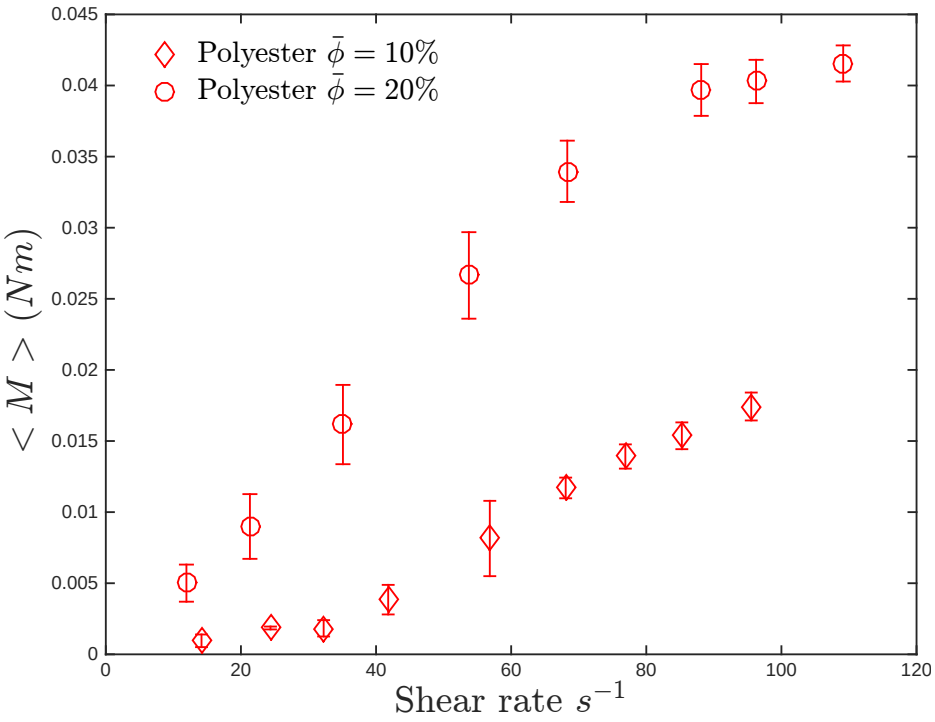

Figure C.4: Measured torques for polyester particles with $\rho_p/\rho = 1.2$ and $\bar{\phi} = 10$ and 20%. Suspending liquid is aqueous glycerine. Error bars represents the combined uncertainty of the measurements.

C.3 Polyester particles with $\rho_p/\rho = 1.2$

Experiments with polyester particles and a density ratio of 1.2 were performed using two different type of suspending liquids: aqueous glycerine and salt water. Both liquids have the same density but differ in viscosity, the former is approximately 7.7 times more viscous than the latter. This allows to study such density ratio at a wider range of Stokes numbers. The salt water density is measured directly with an hydrometer, while the viscosity is inferred from the work of Dessauges et al. (1980); Mao and Duan (2008) and Mao and Duan (2009) and considering a molality of 5.309 mol/Kg.

Figures C.4 and C.5 show the measured torques for loading fractions of 10 and 20% with aqueous glycerine and salt water as the suspending liquid, respectively. Visualization of the flows indicates that for the case with aqueous glycerine as the suspending liquid, the particles never reach the test section for $\bar{\phi} = 10\%$ and for $\bar{\phi} = 20\%$ the particles seem to reach the test section for shear rates higher than 50 s^{-1}.

For the case with salt water, the particles reach the test section at shear rates higher than 80 s^{-1} for $\bar{\phi} = 10\%$ and 35 s^{-1} for $\bar{\phi} = 20\%$. The measured torques don't increase linearly with the shear rate.

Figure C.6 show the measured torques as a function of shear rate for higher loading fractions of 30, 40, and 50%, and aqueous glycerine as the suspending liquid. The torques show a drop for shear

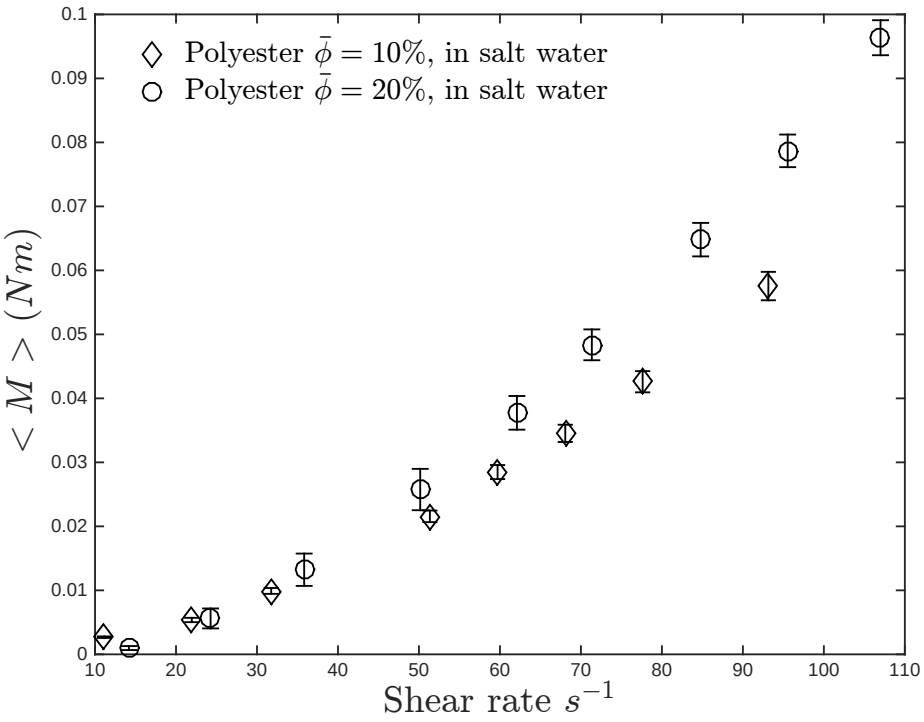

Figure C.5: Measured torques for polyester particles with $\rho_p/\rho = 1.2$ and $\bar{\phi} = 10$ and 20%. Suspending liquid is salt water. Error bars represents the combined uncertainty of the measurements.

rates higher than 40 s^{-1}. For loading fractions of 40 the torques reach a plateau for shear rates higher than 80 s^{-1}, and for the case with $\bar{\phi} = 30\%$ the torques start increasing again for shear rates higher than 80 s^{-1}, mean while for 50% the torques only continue to decrease with the shear rate.

Figure C.7 show the measured torques as a function of shear rate for higher loading fractions of 30, 40, and 50%, and salt water as the suspending liquid. Similarly to the measured torques using aqueous glycerine as the suspending liquid, the torques using salt water show a drop for shear rates higher than 40 s^{-1}. For $\bar{\phi} = 50\%$ the torques continue to decrease, while for $\bar{\phi} = 40$ and 30% the torques start increasing again for shear rates higher than 80 s^{-1}

Figure C.8 shows the normalized torques for all the loading fractions tested with the exception of $\bar{\phi} = 10\%$ because for such low loading fractions, visualization of the flow shows no presence of particles in the test section. For loading fraction of 20% the normalized torques decrease with Stokes number rather than increase. For the rest of the loading fractions the ratio of torques behave in the same way as for the case with $\rho_p/\rho = 1.4$ and water as the suspending liquid.

Figure C.9 presents the normalized torques for polyester particles immersed in salt water with a density ratio of 1.2 for all the loading fractions tested. Only the cases where the particles reach the test section are shown. Unlike the case with same density ratio but with aqueous glycerine as the suspending liquid, the ratio of torques for $\bar{\phi} < 30\%$ increases with shear rate. For the rest loading fractions (30, 40, and 50%) the normalized torques exhibit the same behavior as for the case

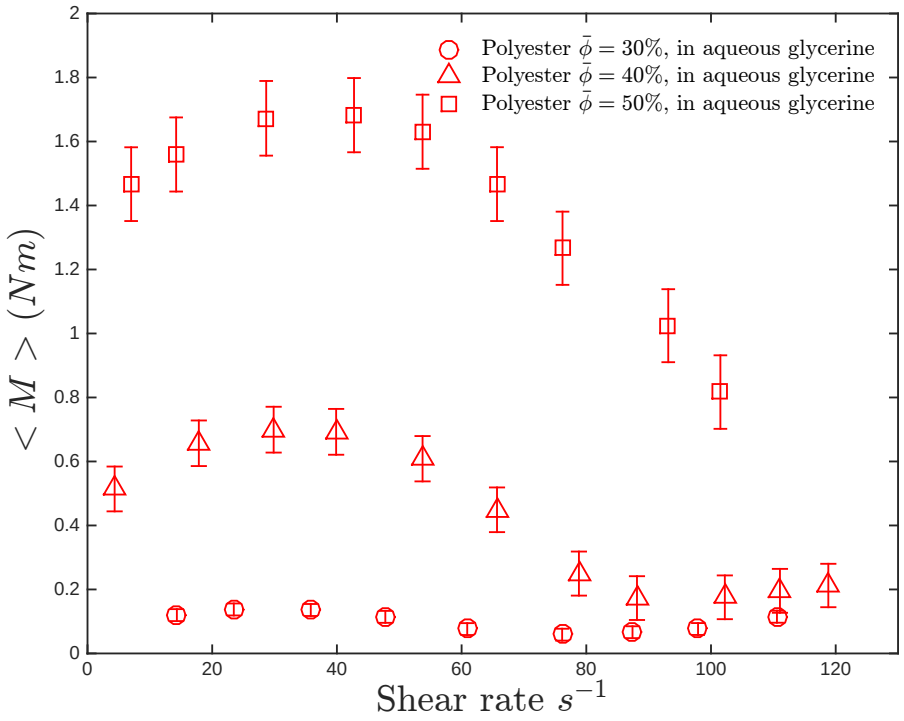

Figure C.6: Measured torques for polyester particles with $\rho_p/\rho = 1.2$ and $\bar{\phi} = 30$, 40, and 50%. Suspending liquid is aqueous glycerine. Error bars represents the combined uncertainty of the measurements.

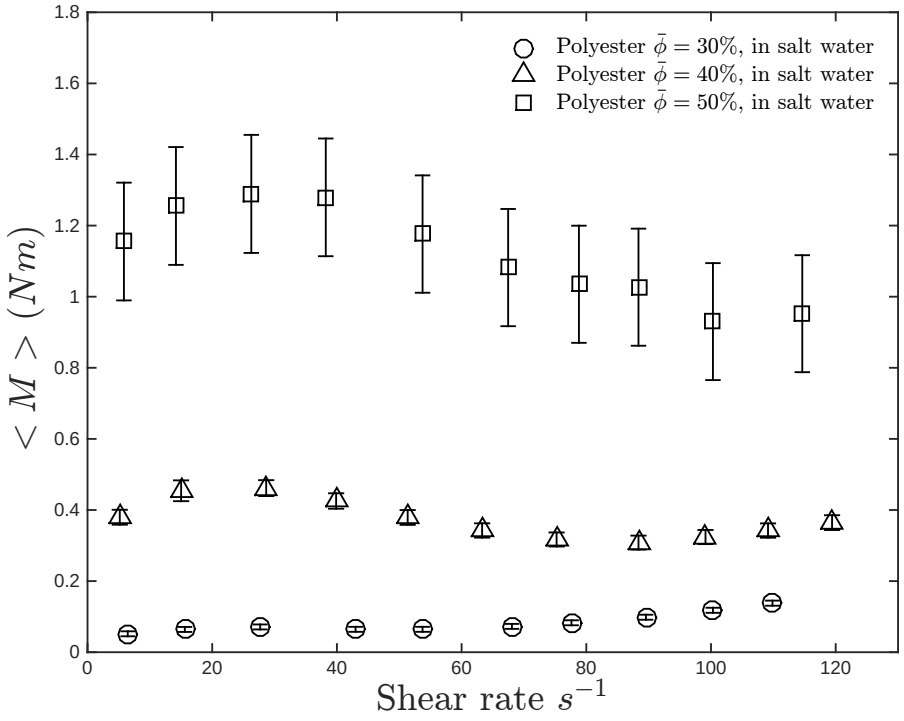

Figure C.7: Measured torques for polyester particles with $\rho_p/\rho = 1.2$ and $\bar{\phi} = 30$, 40, and 50%. Suspending liquid is salt water. Error bars represents the combined uncertainty of the measurements.

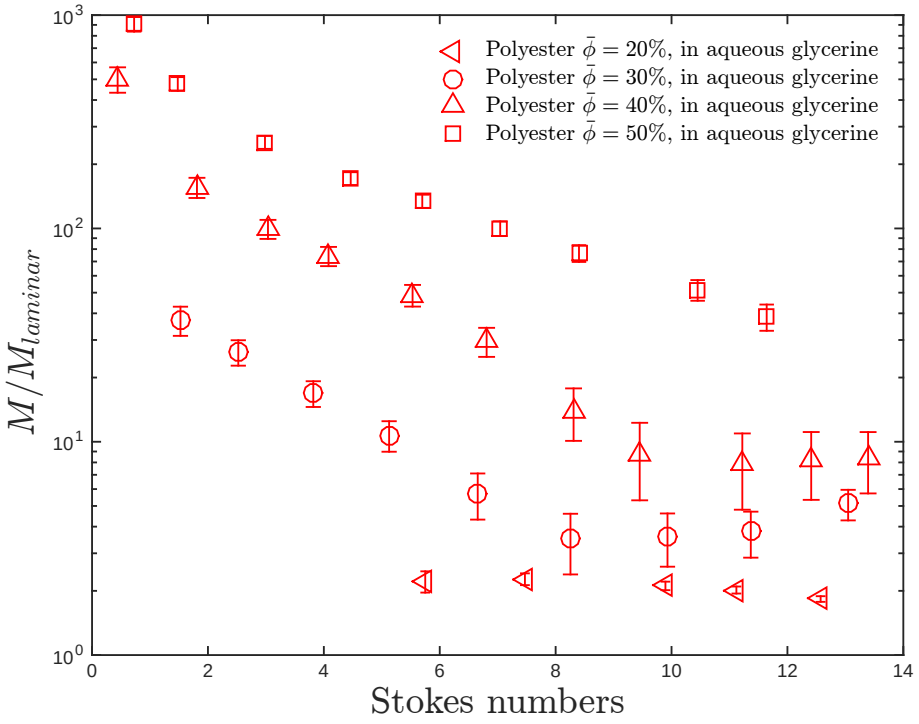

Figure C.8: Normalized torques for polyester particles with $\rho_p/\rho = 1.2$ and $\bar{\phi} = 20, 30, 40$, and 50%. The suspending liquid is aqueous glycerine. Only the results for the case where the particles reach the test section are shown. Error bars represents the combined uncertainty of the measurements.

with same density ratio but aqueous glycerine as the suspending liquid, and as for the case with $\rho_p/\rho = 1.4$ and water as the suspending liquid.

C.4 Direct comparison between same particles but different density ratios

Figure C.10 presents the normalized torques for $\bar{\phi} = 10$ and 20%, and for $\rho_p/\rho = 1.2$, and $\rho_p/\rho = 1.4$. The normalized torques for the case with aqueous glycerine as the suspending liquid is one order of magnitude lower than for the case with salt water as the suspending liquid, even though the density ratios are the same. The reason for this big difference is due to the presence of hydrodynamic effects. Figure C.11 shows the measured torques normalized by the corresponding laminar torques as a function of the modified gap Reynolds number which is defined in Section 2.4 for pure fluid and for loading fractions of 10% and 20% with water, salt water, and aqueous glycerine. For these low loading fractions, the visualizations show no presence of particles at the test section for the case with aqueous glycerine as the suspending liquid and $\bar{\phi} = 10\%$, and no presence of particles for water and salt water for shear rates lower than 65 and 85 s^{-1} and $\bar{\phi} = 20\%$, respectively. Therefore, the measured torques for these cases correspond to just the liquid. Deviation from the laminar

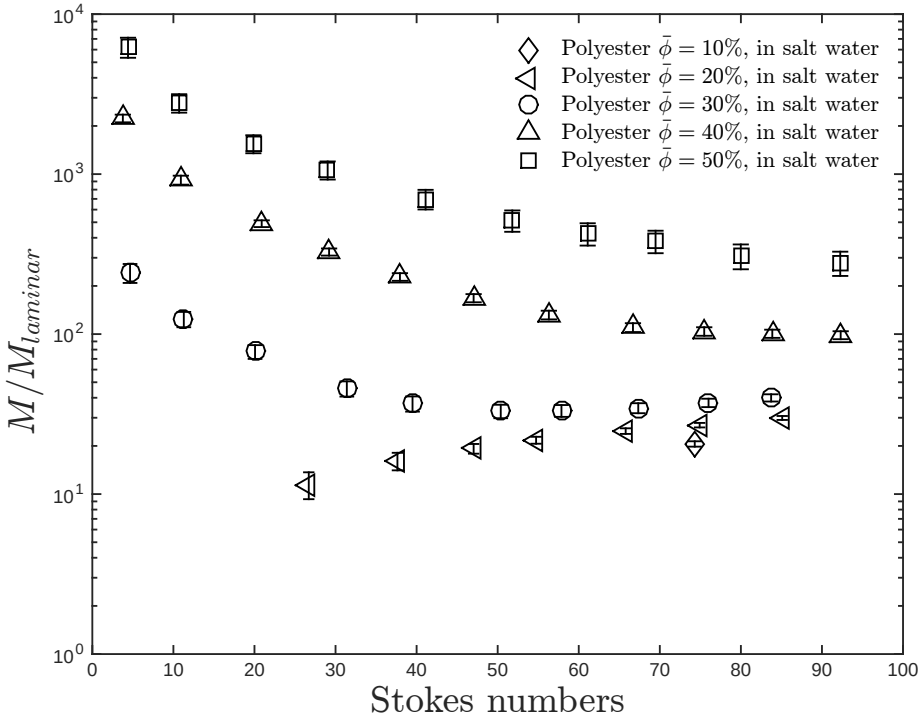

Figure C.9: Normalized torques for polyester particles with $\rho_p/\rho = 1.2$ and $\bar{\phi} = 20, 30, 40$, and 50%. The suspending liquid is salt water. Only the results for the case where the particles reach the test section are shown. Error bars represents the combined uncertainty of the measurements.

behavior is observed for the case with water and salt water, meanwhile for aqueous glycerine the normalized torques are closer to the laminar behavior; however the normalized torques for lower modified gap Reynolds numbers exhibit larger scatter. This is due to an increase in the uncertainty in the measurements of such low torques but as the torques increase with shear rate, the scatter decreases and a clear laminar behavior is observed. Figure C.12 shows the normalized torques as a function of Re_b^* for the present and previous pure fluid measurements from Koos (2009). Notice how the scatter observed for the torque measurements of $\bar{\phi} = 10$ and 20% in aqueous glycerine lies within the scatter observed in the previous measurements of Koos (2009). Therefore the experiments with water and salt water are likely to be affected by the presence of hydrodynamic instabilities.

Figure C.13 shows the normalized torques for loading fraction of 30% for $\rho_p/\rho = 1.4$ and $\rho_p/\rho = 1.2$. For the latter case, results using aqueous glycerine and salt water are shown. The behavior is the same for the three cases shown but the magnitudes do not coincide. For the experiments with $\rho_p/\rho = 1.2$ and aqueous glycerine as the suspending liquid, the ratio of torques is lower than for the case with the same density but higher Stokes number (salt water as the suspending liquid). Aside from the possible presence of hydrodynamics effects for the cases with higher Stokes numbers, the reason for these differences also include the effects of centripetal forces. Visualizations of the flow show that for the experiments with aqueous glycerine and water as the suspending liquid,

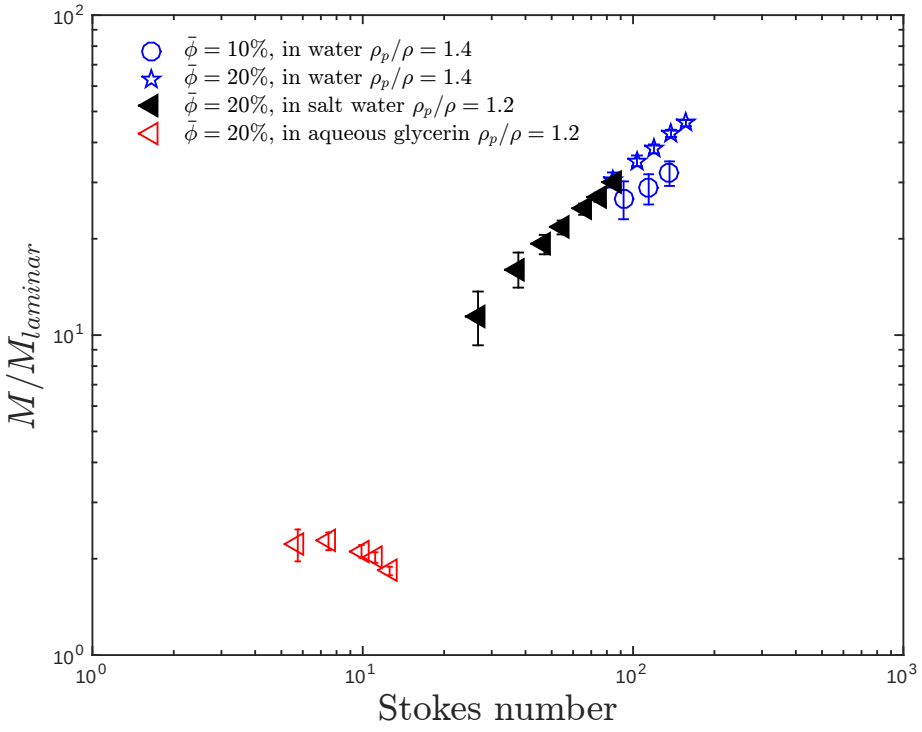

Figure C.10: Comparison between the $M/M_{laminar}$ for $\rho_p/\rho = 1.4$ and $\rho_p/\rho = 1.2$ and $\bar{\phi} = 10$ and 20%. Only the cases with particles present in the test section are shown.

the polyester particles move away from the inner wall. For the experiments with salt water, some particles stay close to the inner wall. This would lead to higher normalized torques but as seen in Figure C.13, the ratio of torques for the case with salt water is lower than the normalized torques for the case with water, where no particles are touching the inner cylinder for high Stokes numbers. The reason for this discrepancy is not clear, one possible explanation is that the hydrodynamic inertial effects present for the case with water as the suspending liquid are more pronounced than in the case with salt water. Further details on the flow visualizations is presented in the next section.

Figure C.14 shows the normalized torques for loading fraction of 40% and density ratios of 1.2 and 1.4. Similar to the case of $\bar{\phi} = 30\%$, the behavior for the three cases is the same and the ratio of torques only differ in magnitude, where the case with aqueous glycerine shows lower normalized torques than the experiments with water and salt water. The same behavior is found for $\bar{\phi} = 50\%$, as shown in Figure C.15.

C.5 Flow visualization for polyester particles

Visualization of the flow using water, salt water, and aqueous glycerine as the suspending liquid and polyester particles are presented in this section. The density ratio for the case with water is 1.4, and for aqueous glycerine and salt water the density ratio is 1.2.

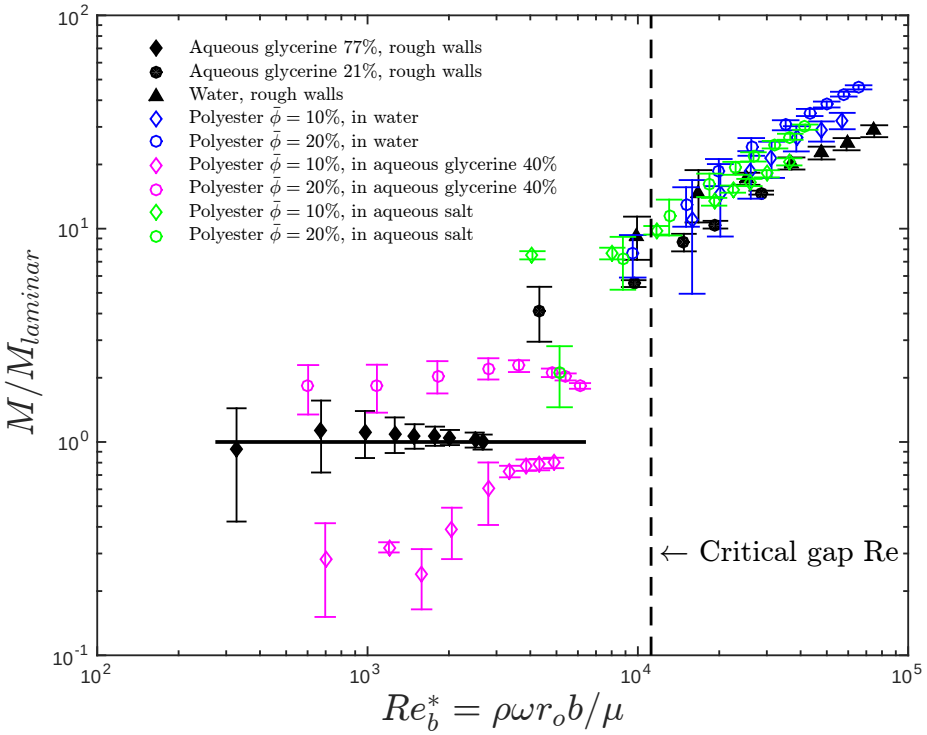

Figure C.11: Normalized torques for pure fluid and for low loading fractions of 10 and 20% where particles are not present in the test section. Vertical dashed line corresponds to the critical modified gap Reynolds number based on the work of Taylor (1936a) and considers the gap width for rough walls.

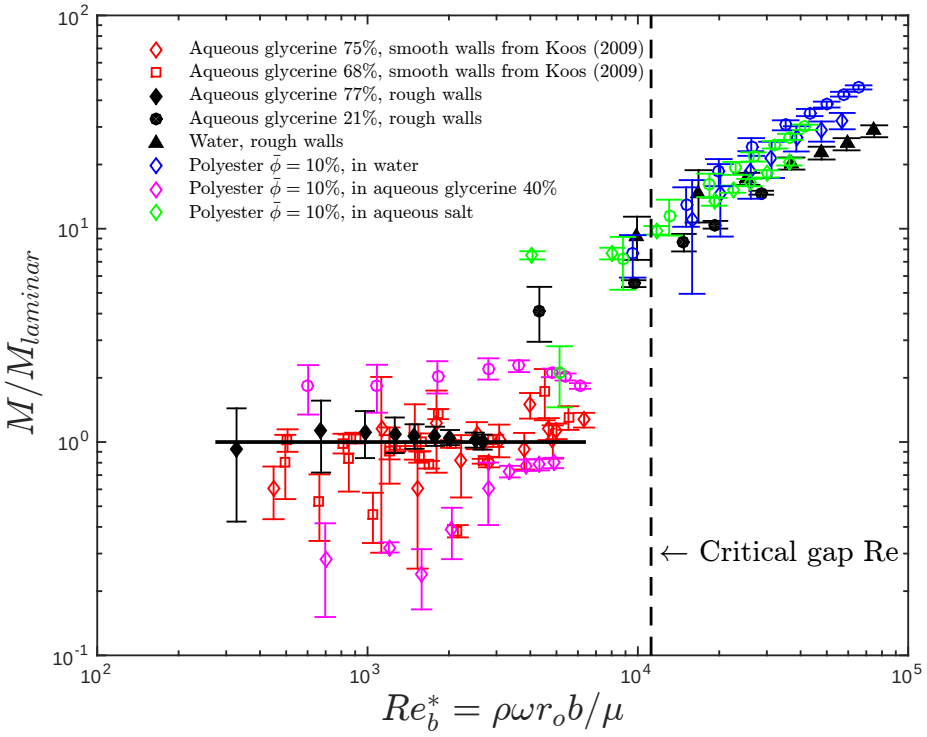

Figure C.12: Previous and present normalized torques for pure fluid and for low loading fractions of 10 and 20% where particles are not present in the test section. The previous torque measurements were done by Koos (2009) and used smooth walls. Vertical dashed line corresponds to the critical modified gap Reynolds number based on the work of Taylor (1936a) and considers the gap width for rough walls.

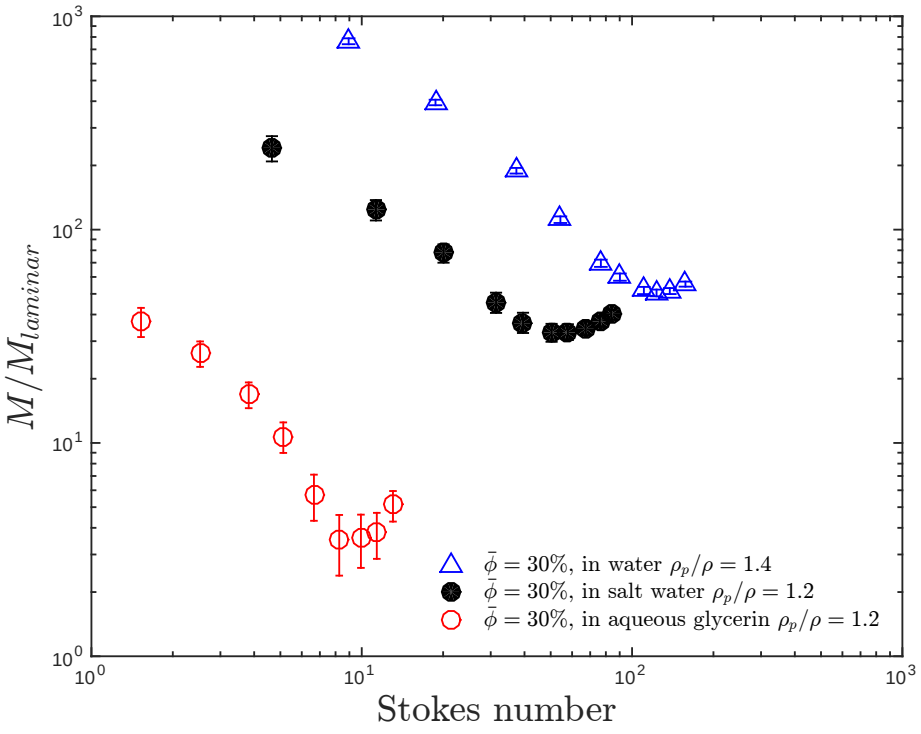

Figure C.13: Normalized torques for polyester particles and $\rho_p/\rho = 1.4$ and, $\rho_p/\rho = 1.2$ as a function of Stokes numbers for $\bar{\phi} = 30\%$. The suspending liquids are water, salt water, and aqueous glycerine.

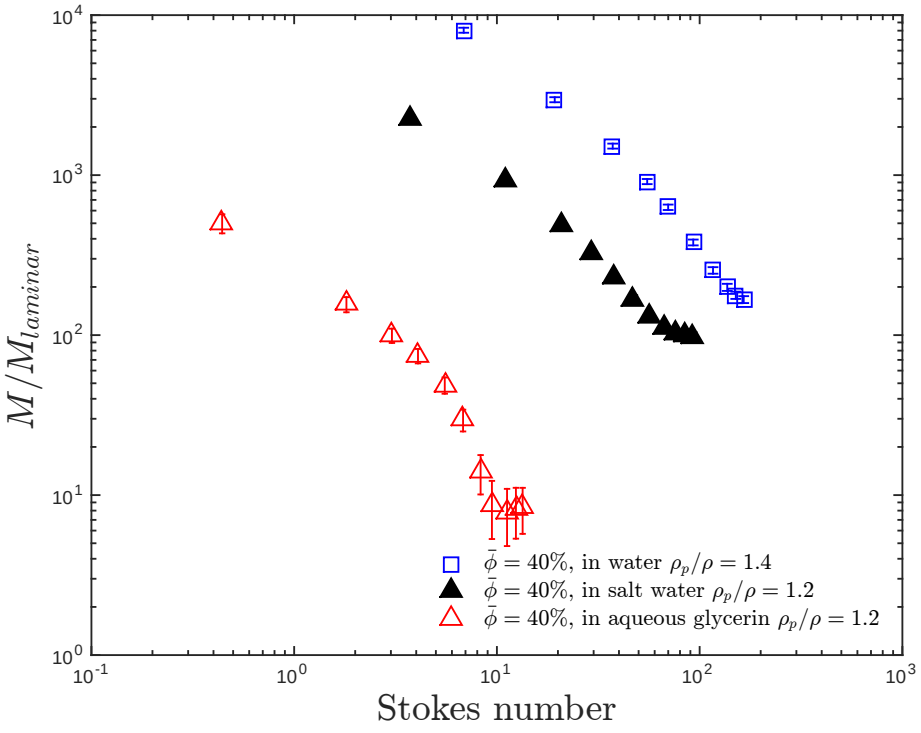

Figure C.14: Normalized torques for polyester particles and $\rho_p/\rho = 1.4$ and, $\rho_p/\rho = 1.2$ as a function of Stokes numbers for $\bar{\phi} = 40\%$. The suspending liquids are water, salt water, and aqueous glycerine.

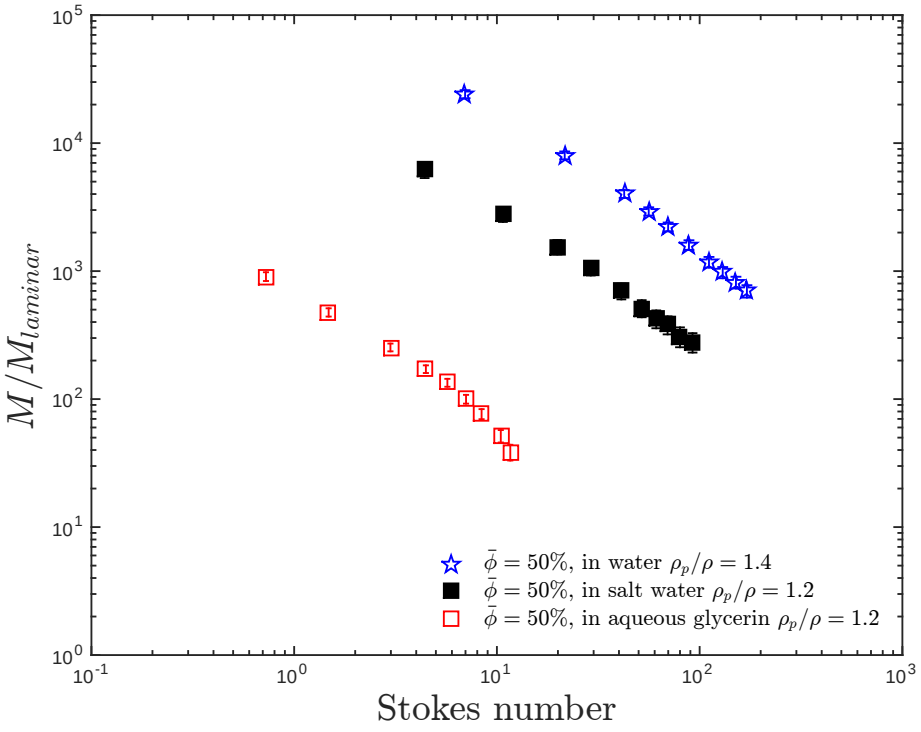

Figure C.15: Normalized torques for polyester particles and $\rho_p/\rho = 1.4$ and, $\rho_p/\rho = 1.2$ as a function of Stokes numbers for $\bar{\phi} = 50\%$. The suspending liquids are water, salt water, and aqueous glycerine.

Visualizations for $\rho_p/\rho = 1.4$

Figure C.16 shows the image sequence corresponding to a loading fraction of 10%, and for a density ratio of 1.4 at different Stokes numbers. The particles reach the test section height above certain Stokes numbers, but unlike the visualizations for polystyrene particles ($\rho_p/\rho = 1.05$) the polyester particles exhibit a radial migration and move towards the outer cylinder. The particles observed in Figure C.16 are not next to the inner cylinder but next to the outer one. Movies at different Stokes number show that the particles are touching the outer cylinder and as Stokes numbers increase, the polyester particles climb the outer wall and exhibit little interaction between each other. Therefore, the torque measurements for these loading fractions correspond to pure fluid measurements with a narrower annular gap in which the width decreases as more particles climb the outer wall.

For a loading fraction of 30%, the polyester particles are next to the inner wall at low Stokes numbers, and move away from the inner wall as Stokes increases. At the highest Stokes numbers there are no particles touching the test cylinder, and all the particles are pushed against the outer wall.

Similar results are found for volume fraction of 40 and 50%, as shown in Figures C.18 and C.19. At the highest Stokes numbers some of the polyester particles are touching the lower part of the test cylinder for $\bar{\phi} = 40\%$, and for $\bar{\phi} = 50\%$ the polyester particles are touching the test cylinder

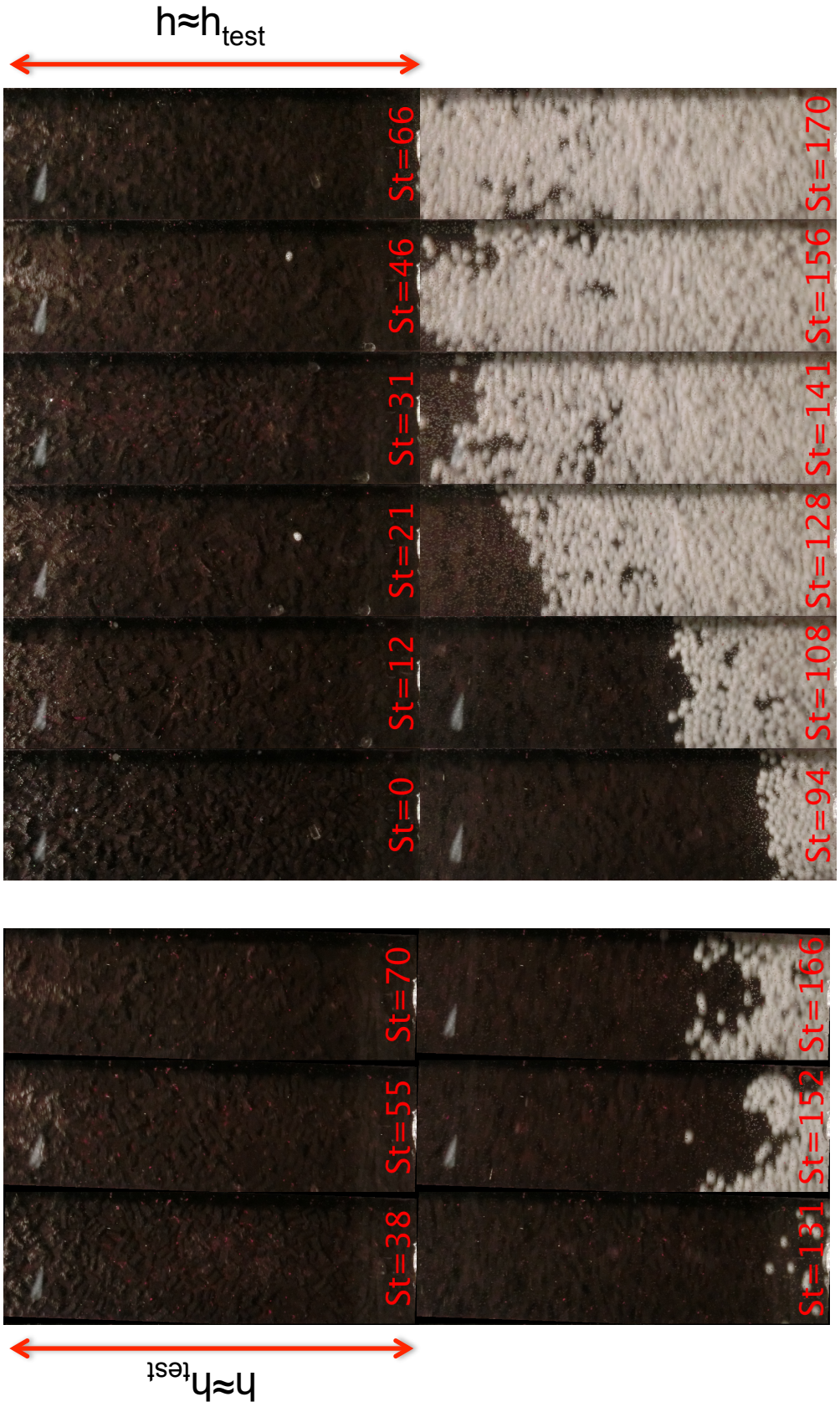

Figure C.16: Image sequence at different Stokes numbers for: (a) $\bar{\phi} = 10\%$ and (b) $\bar{\phi} = 20\%$. The density ratio for (a) and (b) is 1.4.

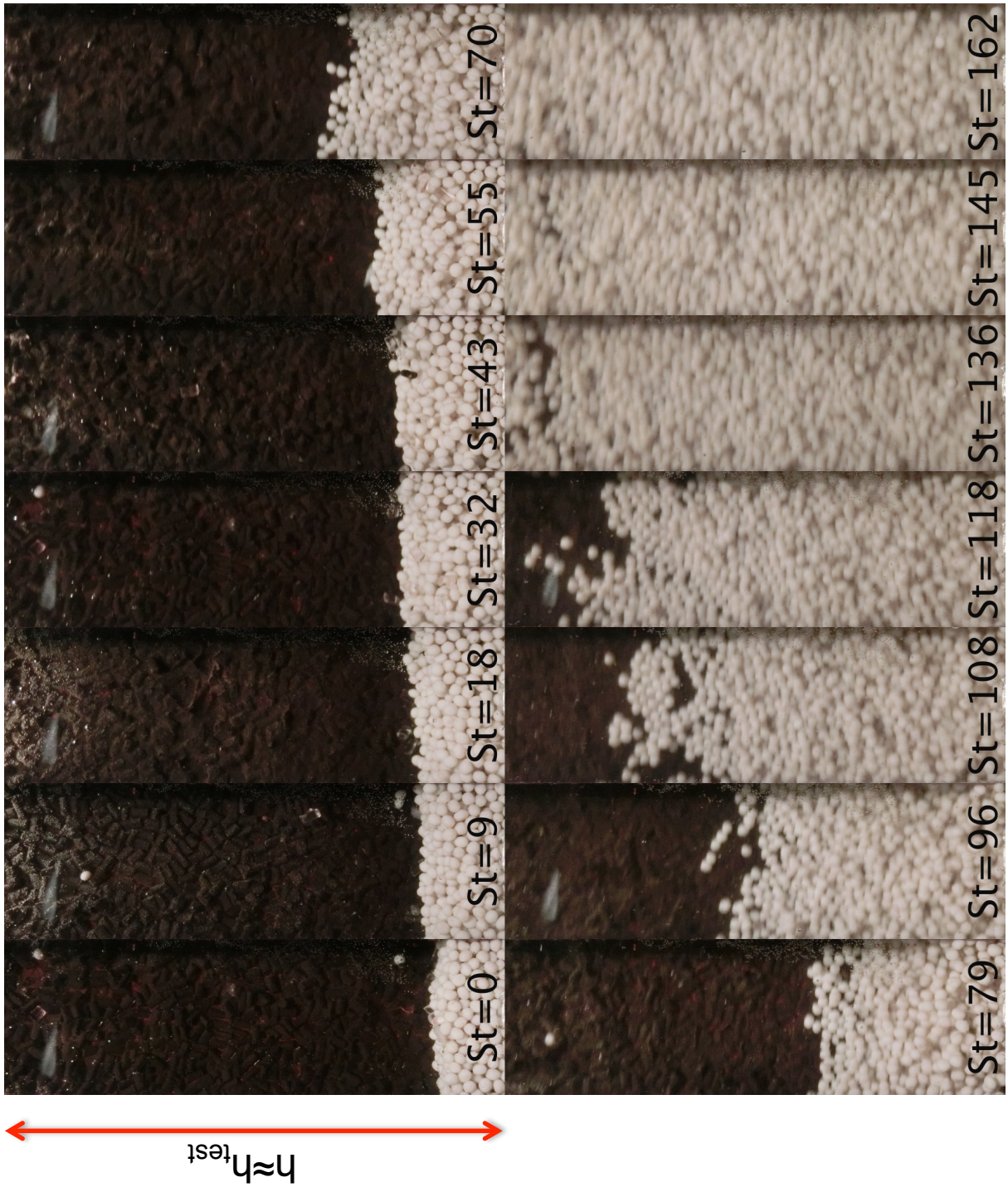

Figure C.17: Image sequence at different Stokes numbers for $\bar{\phi} = 30\%$. The density ratio is 1.4.

but their packing seem to have diminished.

Visualizations for $\rho_p/\rho = 1.2$

Figure C.20 shows the flow visualization for $\bar{\phi} = 10\%$, and a density ratio of 1.2 but different suspending liquids. The aqueous glycerine is 7.7 times more viscous than the salt water, leading to lower Stokes numbers. Only the images corresponding to the highest Stokes numbers tested for this loading fraction is shown. For the case with aqueous glycerine the particles never reach the test section, and for the case with salt water some particles climb the outer wall but do not touch the inner test section. The images for this visualization are blurry due to the opacity of the interstitial liquid, and the particles distance from the inner wall.

Figure C.21 shows the flow visualization for $\bar{\phi} = 20\%$ and a density ratio of 1.2 with different suspending liquids. For both cases the particles never touch the test section. When the suspending liquid is salt water, the presence of particles on the outer wall are indicated by the blurry white background on the pictures. When the polyester particles are touching the test section their image is sharp.

Figure C.22 shows the flow visualization for $\bar{\phi} = 30\%$ and $\rho_p/\rho = 1.2$ with salt water as the suspending liquid. At low Stokes numbers the particles do not exhibit strong radial migration but as Stokes numbers increases the particles begin to move away from the inner test section. However, not all the particles move away. This can be observed by the sharpness of the particles' images.

Figure C.23 shows the flow visualization for $\bar{\phi} = 30\%$ and $\rho_p/\rho = 1.2$ with aqueous glycerine as the suspending liquid. Similar to the case with salt water as the suspending liquid, the particles remain in contact with the test section wall at low Stokes numbers and migrate radially towards the outer cylinder. Unlike the case with salt water, the particles for this case stop touching the test cylinder wall at higher Stokes numbers. This results in a significant decrease of particle interactions because the particles are mainly pushed against the outer cylinder and follow the outer cylinder velocity.

Figure C.24 shows the flow visualization for $\bar{\phi} = 40\%$ and $\rho_p/\rho = 1.2$ with salt water as the suspending liquid. The radial migration of the particles makes the height reach by the particles next to the test section look constant. The way the particles migrate is similar to the one observed for the same parameters but $\bar{\phi} = 30\%$.

The radial migration for the same density ratio but more viscous fluid is significantly larger, as can be observed in Figure C.25. The majority of the particles are pushed against the outer cylinder and fewer particles remained touching the test section at the highest Stokes number.

Figure C.26 and C.27 show the flow visualization for $\bar{\phi} = 50\%$ and $\rho_p/\rho = 1.2$ with salt water and aqueous glycerine as the suspending liquid, respectively. Similar to the results found for this high loading fraction and $\rho_p/\rho = 1.4$, the particles packing seem to decrease with increasing Stokes

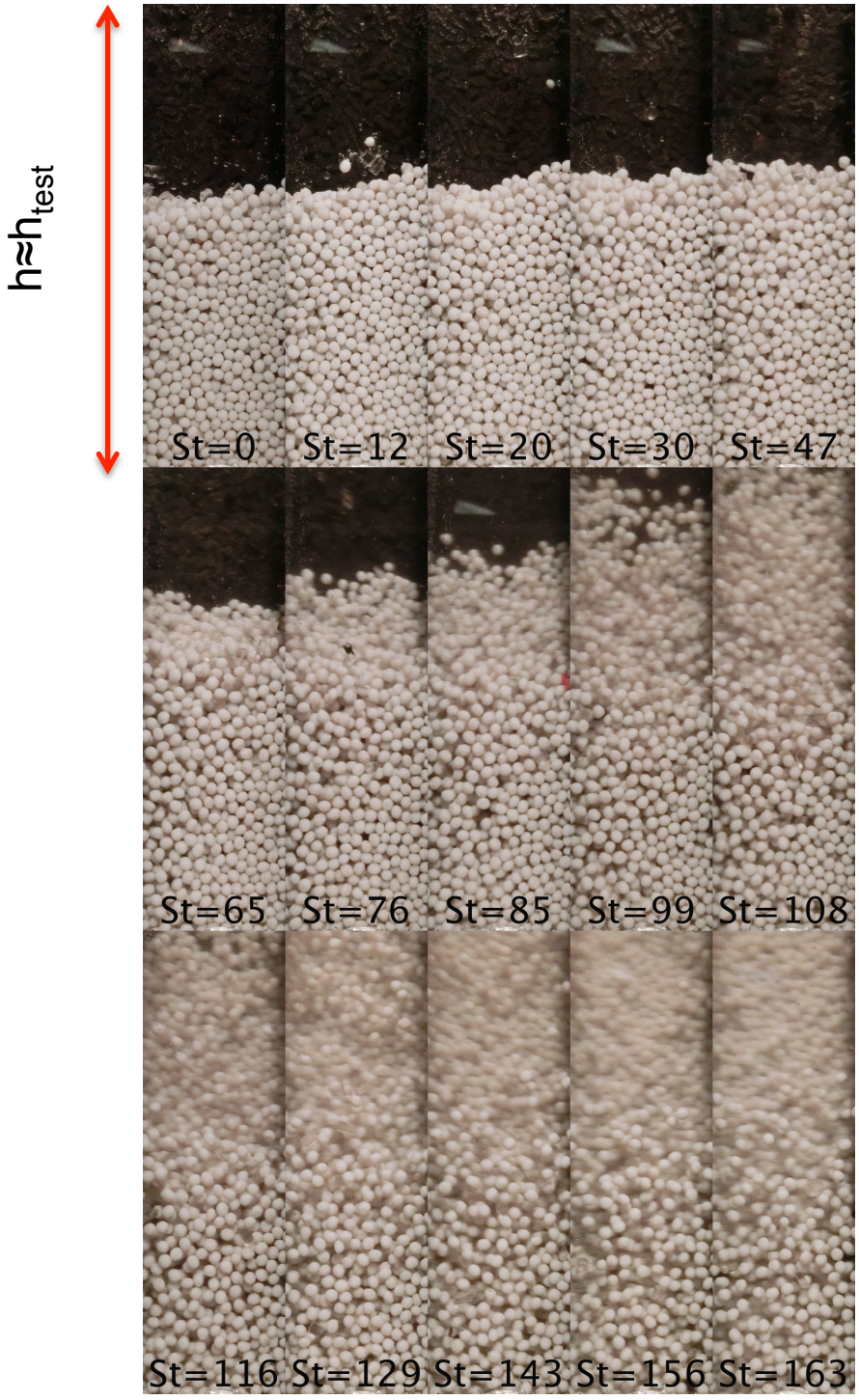

Figure C.18: Image sequence at different Stokes numbers for $\bar{\phi} = 40\%$. The density ratio is 1.4.

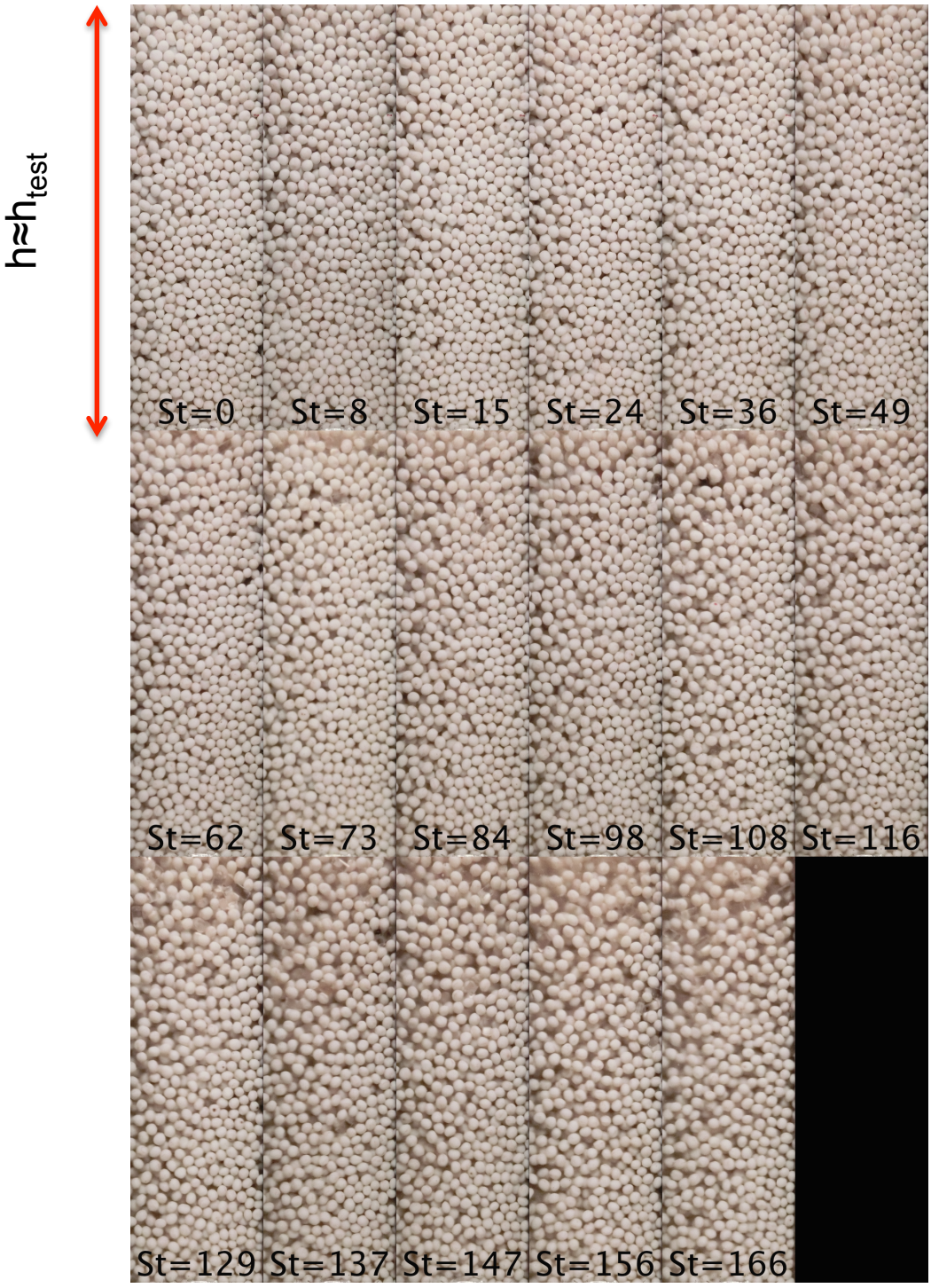

Figure C.19: Image sequence at different Stokes numbers for $\bar{\phi} = 50\%$. The density ratio is 1.4.

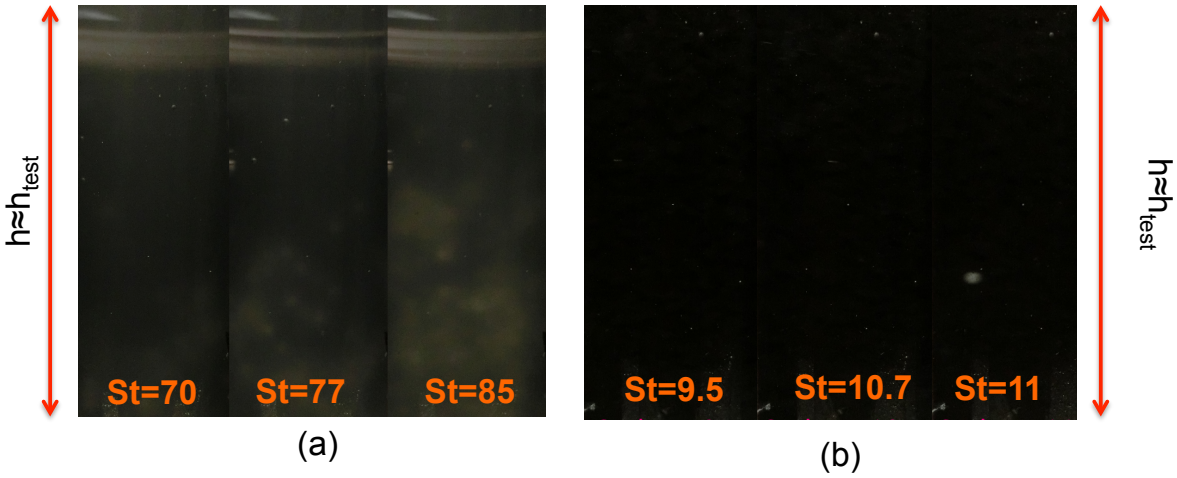

Figure C.20: Image sequence at different Stokes numbers for $\bar{\phi} = 10\%$. The density ratio is 1.2. (a) suspending liquid is salt water and (b) suspending liquid is aqueous glycerine.

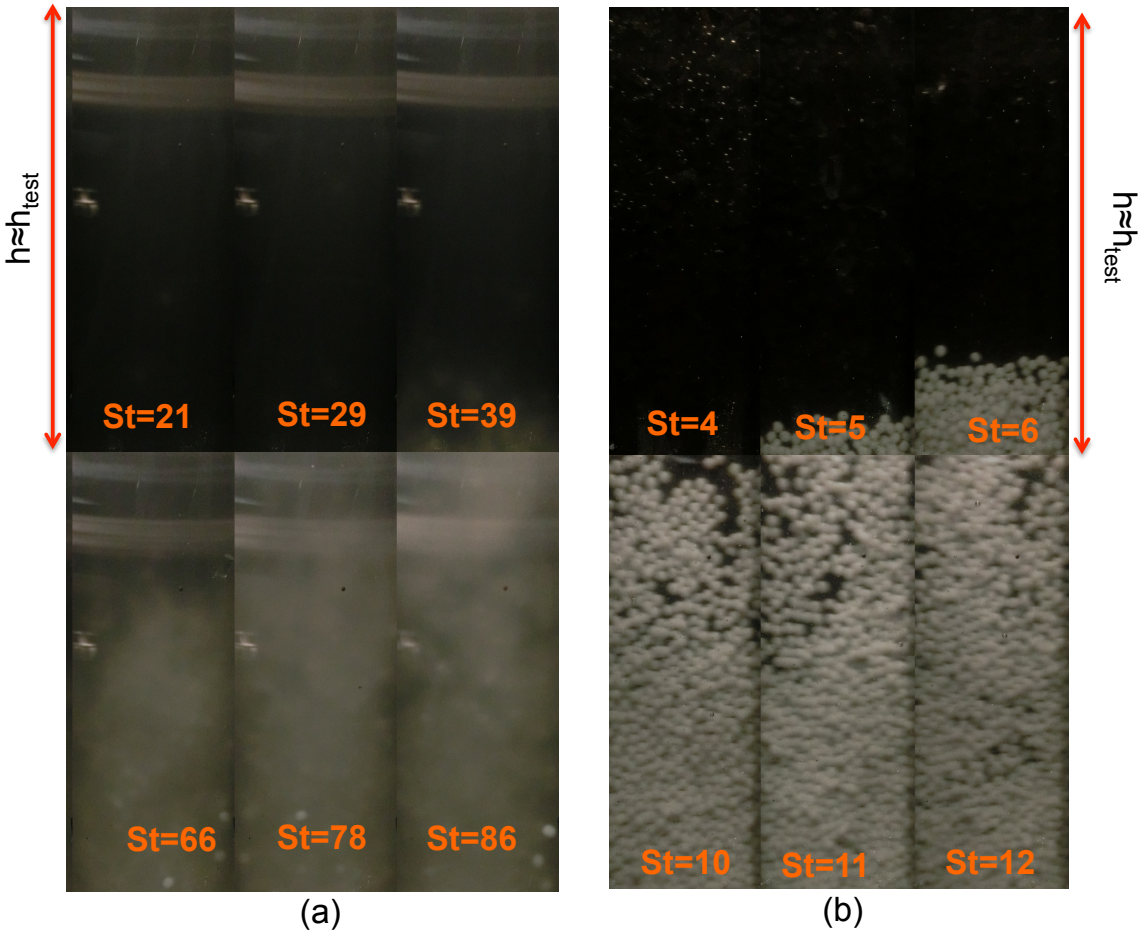

Figure C.21: Image sequence at different Stokes numbers for $\bar{\phi} = 20\%$. The density ratio is 1.2. (a) suspending liquid is salt water and (b) suspending liquid is aqueous glycerine.

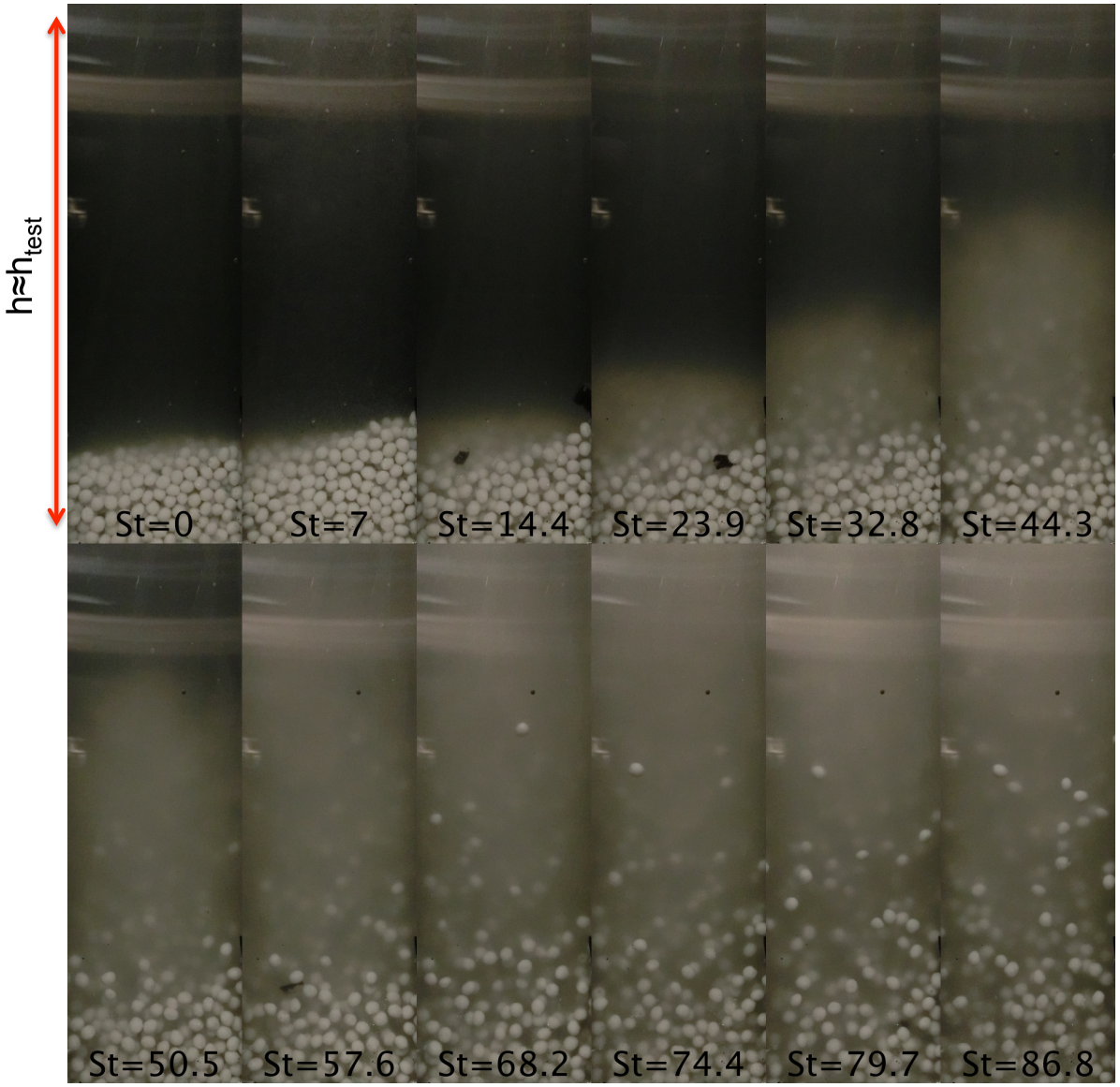

Figure C.22: Image sequence at different Stokes numbers for $\bar{\phi} = 30\%$. The density ratio is 1.2 and the suspending liquid is salt water.

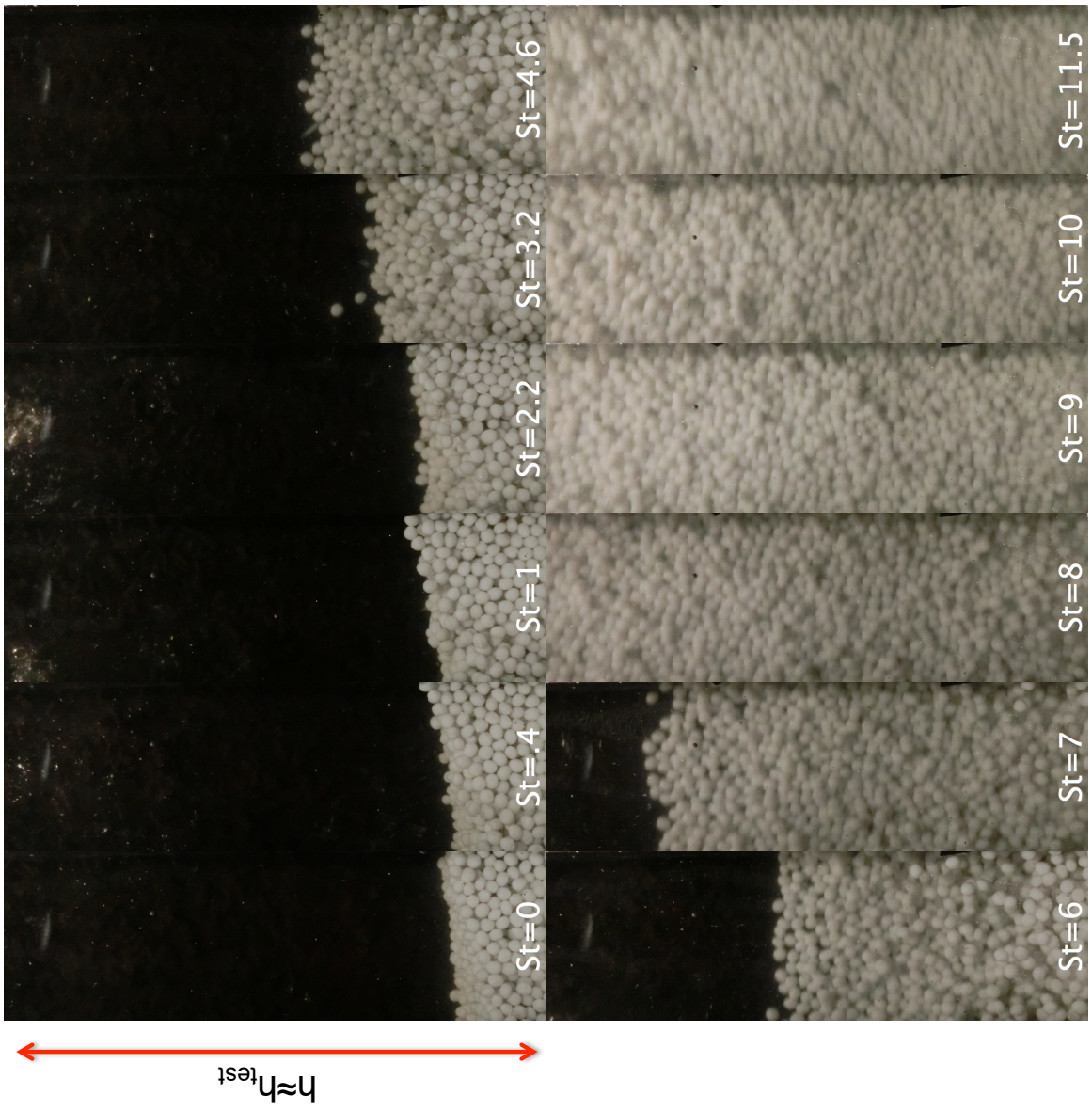

Figure C.23: Image sequence at different Stokes numbers for $\bar{\phi} = 30\%$. The density ratio is 1.2 and the suspending liquid is aqueous glycerine.

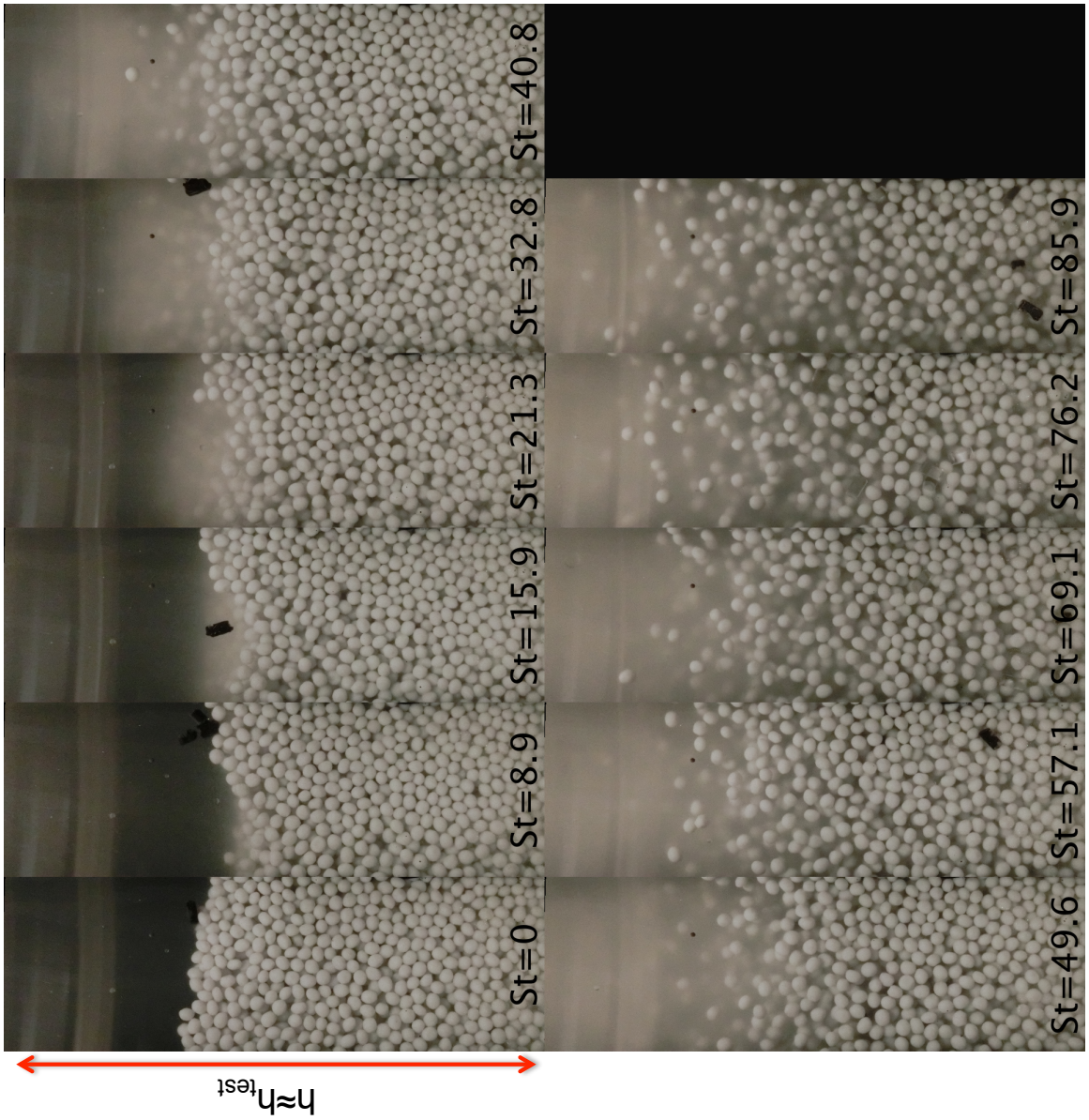

Figure C.24: Image sequence at different Stokes numbers for $\bar{\phi} = 40\%$. The density ratio is 1.2 and the suspending liquid is salt water.

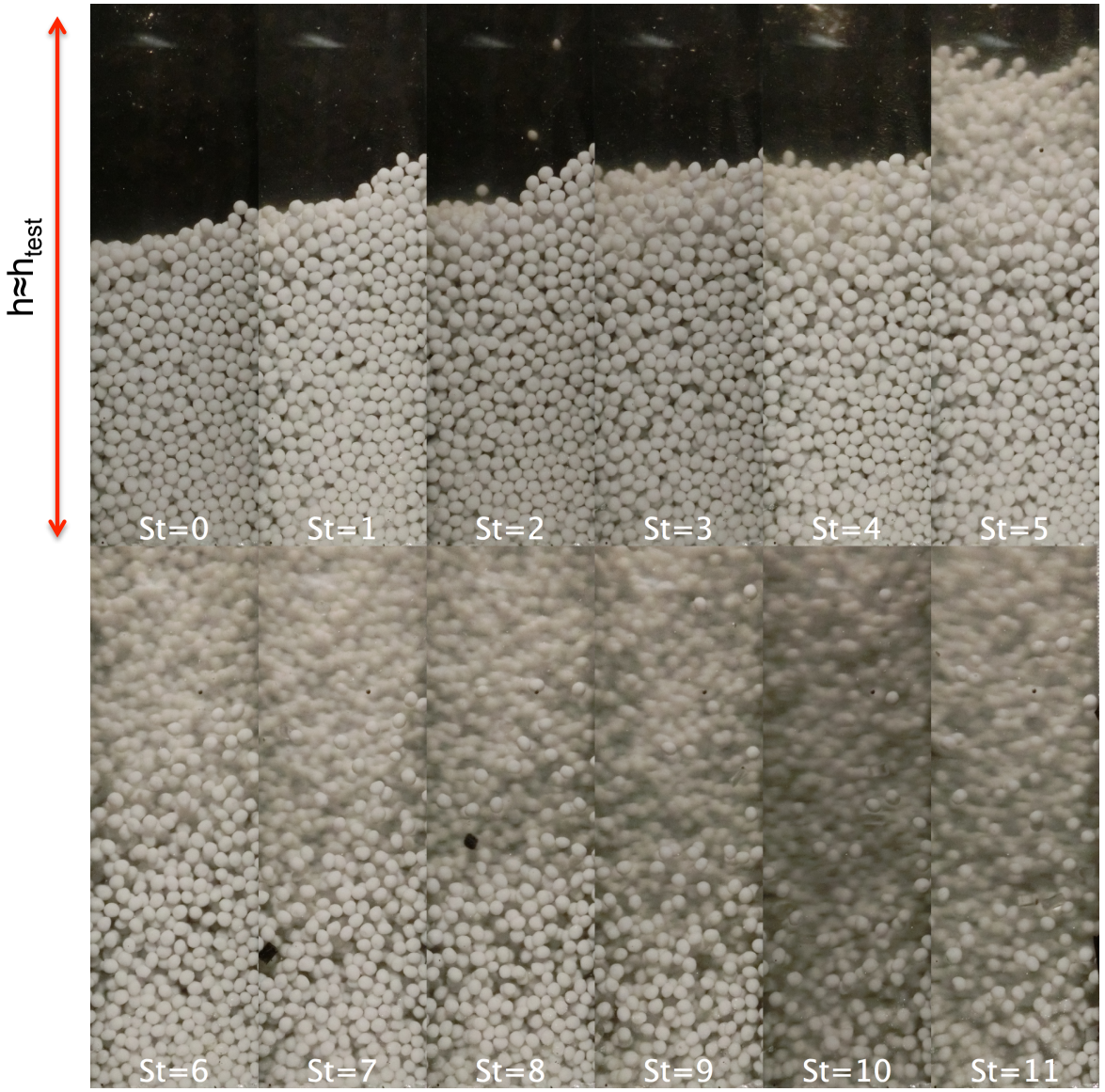

Figure C.25: Image sequence at different Stokes numbers for $\bar{\phi} = 40\%$. The density ratio is 1.2 and the suspending liquid is aqueous glycerine.

numbers and the particles are touching the test section.

C.6 Discussion

Because of the constraint on the visualization window height and the presence of radial migration, it is not possible to determine the effective volume fraction for these liquid-solid flows. What is possible to determine is the lack of particles next to the inner wall for loading fractions of 10 and 20% for the three cases studied. Through the flow visualization is possible to propose some reasons for the measured torque behavior. For the experiments with aqueous glycerine as the suspending liquid, the normalized torques are considerably lower than the normalized torques found for the same density ratio but with a less viscous liquid (salt water). Aside from having lower Stokes numbers and thus lower Reynolds stress, the flow visualization for this case show that the particles radial migration is considerably larger than for the case with salt water. This leads to measurements of pure fluid rather than measurements of the mixture for most of the Stokes numbers tested. This explains in part the lower normalized torques measured for the same density ratio and lower Stokes numbers. There is also the possibility that the experiments with higher Stokes numbers but same density ratio, are affected by hydrodynamic instabilities that increase the measured torques.

For the case with larger density ratio ($\rho_p/\rho = 1.4$) the particles also show a very similar significant radial migration than the one observed for the experiments with aqueous glycerine. The reason for this is not completely clear but one possible reason could be that even when the experiments with lower density ratio would experience lower centripetal forces, the viscosity of the fluid is higher (approximately 13.6 times higher than water) and therefore, the drag force too. Higher drag forces would push the particles towards the outer cylinder if the liquid itself is being pushed towards that direction. The reason why the experiments with salt water do not exhibit a strong radial migration might be because the particles in these experiments experience lower centripetal forces than for the case with $\rho_p/\rho = 1.4$ and the drag force would be less than for the case with the same density ratio but more viscous fluid.

The visualizations for the highest loading fraction of 50% does not show a strong difference in particle concentration and behavior among the three cases studied. However, the normalized torques does not have the same values. The reason for these differences is not clear, although the differences are less pronounced than the differences found for the lower volume fractions. It is possible that the salt water viscosity that was inferred from the work of Dessauges et al. (1980); Mao and Duan (2008) and Mao and Duan (2008) might not be completely accurate.

From the movies of the flow, the particle agitation next to the test section wall for the case with salt water seems to be higher than the one observed for the other two cases ($\rho_p/rho = 1.4$ and water as the suspending liquid, and $\rho_p/\rho = 1.2$ with aqueous glycerine as the suspending liquid).

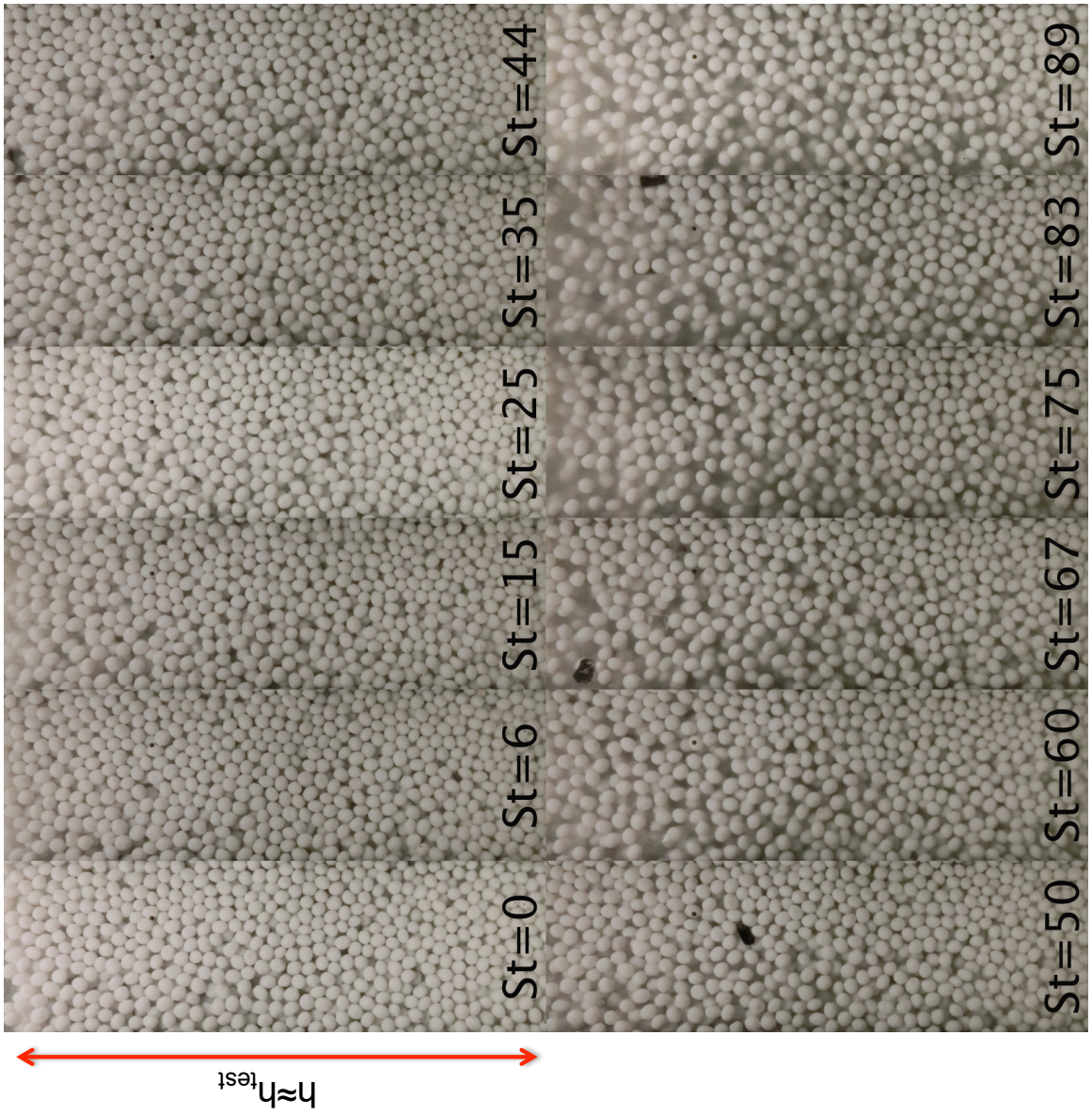

Figure C.26: Image sequence at different Stokes numbers for $\bar{\phi} = 50\%$. The density ratio is 1.2 and the suspending liquid is salt water.

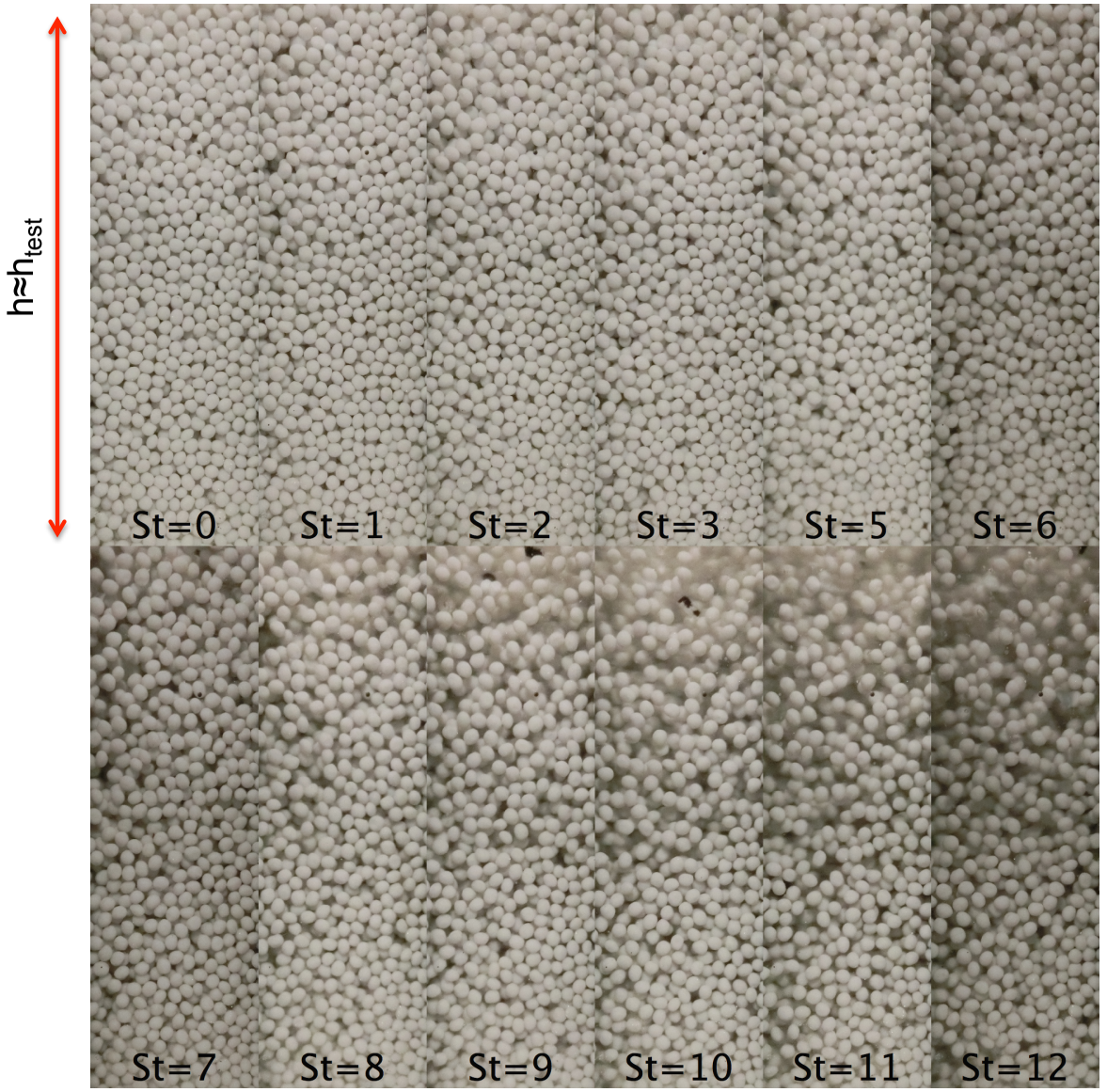

Figure C.27: Image sequence at different Stokes numbers for $\bar{\phi} = 50\%$. The density ratio is 1.2 and the suspending liquid is aqueous glycerine.

This would lead to higher normalized torques not only because of the particle interactions but also because the effective volume fraction is higher. However, the normalized torques for salt water are lower than for the case with $\rho_p/\rho = 1.4$. The reason for this is not clear and it might be an error in the calculation of the salt water viscosity.